

CLOTHO: A Large-Scale Internet of Things based Crowd Evacuation Planning System for disaster management

Xialong Xu, Lei Zhang, Stelios Sotiriadis, Eleana Asimakopoulou, Maozhen Li, Nik Bessis

Abstract—In recent years, different kinds of natural hazards or man-made disasters happened that were diversified and difficult to control with heavy casualties. In this work, we focus on the rapid and systematic evacuation of large-scale densities of people after disasters in order to reduce loss in an effective manner. The optimal evacuation planning is a key challenge and becomes a hotspot of research and development. We design our system based on an Internet of Things (IoT) scenario that utilizes a mobile Cloud computing platform in order to develop the Crowd Lives Oriented Track and Help Optimization system (CLOTHO) that is an evacuation planning system for large-scale densities of people in disasters. CLOTHO includes the mobile terminal (IoT side) for data collection and the Cloud backend system for storage and analytics. We build our solution upon a typical IoT/fog disaster management scenario and we propose an IoT application based on an evacuation planning algorithm based on the artificial potential Field (APF), which is the core of CLOTHO. APF is conceptualized as an IoT service, and can determine the direction of evacuation automatically according to the gradient direction of the potential field, suitable for rapid evacuation of large population. People are usually in panic, which easily causes the chaos of evacuation and brings secondary disasters. Based on APF, we propose the evacuation planning algorithm based on artificial potential field with relationship attraction (APF-RA). APF-RA guides the evacuees with relationship to move to the same shelter as much as possible, to calm evacuees and realize a more humanitarian evacuation. The experimental results show that CLOTHO (using APF and APF-RA) can effectively improve convergence rate, shorten the evacuation route length and evacuation time, and make the remaining capacity of the surrounding shelters balanced. Furthermore, CLOTHO aims to bring evacuees to the same shelter if possible and appropriate.

Index Terms—Internet of Things, evacuation planning, artificial potential field, relationship attraction, disaster

1 INTRODUCTION

Disasters, no matter natural hazards or man-made disasters happened randomly, which means in many situations they are difficult to predict and control. In recent years, it seems that serious disasters happened even more frequently, involving widespread human, material, economic or environmental losses and impacts. In 2005, Hurricane Katrina swept the coast of Florida and the Gulf of Mexico, killed more than 1800 people, and caused millions of people homeless and great economic losses of more than 340 billion US dollars. In 2011, the magnitude-9.0 Tohoku-Oki earthquake off the eastern coast of Japan was one of the largest recorded earthquakes in history. It triggered a devastating tsunami that killed more than 20,000 people and an ongoing nuclear disaster at the Fukushima Daiichi power plant. The number of evacuees was more than 10 million. In 2015, A xylene facility leaked oil and caught fire, which led to blasts and a fire at three nearby oil storage tanks at Tenglong Aromatic Hydrocarbon (Zhangzhou) Co. Ltd. on the Gulei Peninsula in Zhangzhou City of southeast China's Fujian Province.

There was a strong sense of quake within a radius of forty to fifty kilometers, and more than 11,000 local residents needed to be evacuated. All above disasters led to a large-scale mass migration refuge behaviors. Rapid and orderly evacuation of the large-scale people after disasters can reduce loss effectively. The efficiently evacuation planning system is the key, which attracts more and more attentions of governments, academia and industry around the world. In addition, the emergence of Fog, Internet of Things (IoT) and Cloud computing highlight new opportunities for disaster management planning and management. IoT allows fast user data collection based on the peoples' smart devices, while Cloud offers the platform and infrastructure for scalable data analytics and storage.

At present, many evacuation planning models have been presented. For example, X. Song et al. [1], [2] proposed an evacuation probability reasoning model based on the Markov decision process, B. Tang et al. [3] presents a Robot-Assisted evacuation scheme and E. Boukas et al. [4] presents an accurate Cellular Automaton simulation model, V.S. Kalogiton et al. [5] presented a dynamic model based on bionics, M. Di Gangi [6] proposed a dynamic distributed evacuation model, L. Chen et al. [7] presented a distributed emergency evacuation guidance framework based on wireless sensor networks, P. Tsai et al. [8] proposed a dynamic event-related network model, and S. Mukherjee et al. [9] presented a population dynamic model based on the Lagrangian method. Many repre-

Xiaolong Xu is with the Nanjing University of Posts and Telecommunications, Nanjing 210003, China, and also with the Chinese Academy of Sciences, Beijing 100093, China (e-mail: xuxl@njupt.edu.cn).

Lei Zhang is with the Nanjing University of Posts and Telecommunications, Nanjing 210003, China (e-mail: xuxl@njupt.edu.cn).

Stelios Sotiriadis is with the University of Toronto (e-mail: s.sotiriadis@utoronto.ca).

Maozhen Li is with the Brunel University (email: Maozhen.Li@brunel.ac.uk).

Eleana Asimakopoulou and Nik Bessis is with the Edge Hill University (e-mail: Nik.Bessis@edgehill.ac.uk).

sentative emergency evacuation planning systems have been designed and built at the same time. For example, M. U. S. Khan et al. [10] presented an evacuation system based on MacroServ for emergency, Y. Iizuka et al. [11] presented a multi-agent-based cooperative emergency evacuation system, P. G. Raj et al. [12] presented a population evacuation system based on distributed mobile sensors, K. Yu et al. [13] presented an intelligent evacuation guidance system based on image recognition, and F. Zhu et al. [14] presented a parallel public transport evacuation system based on the Artificial societies, Computational experiments, and Parallel execution (ACP) approach. EvacSys [15] is a typical evacuation system based on Cloud computing.

For solving the evacuation planning problem in disasters, the following difficulties need to be overcome:

1. When a disaster happens, the evacuees in the affected area are usually in a state of fear, tension and feelings of helplessness due to the untimely information dissemination and guidance, which affects evacuees' judgments. The herd mentality and unorganized evacuation may cause the congestion of traffic and the imbalance of shelters, which delays the valuable evacuation time. Easy and automatic evacuation (e.g. based on automated IoT data collection solutions and simple to use mobile applications) can assist in this direction.
2. None of current evacuation planning schemes take the psychological factor of human into consideration in disasters or use the interpersonal relationships to achieve the humanitarian evacuation. In fact, it is important to achieve to appease the feelings of refugees as much as possible to avoid chaos when the disaster happens. In short, the humanitarian evacuation can realize the orderly evacuation and maintain the mental stability of the evacuees. Order can be maintained with the use of an effective IoT based algorithm.
3. There are many factors influencing the evacuation planning, such as the locations of shelters and evacuees, the traffic situation and the intentions of evacuees, etc. However, the current evacuation planning systems usually consider certain aspects of factors, which affects the efficiency of evacuation or lacks of practicability. In this direction, an IoT based system can be extremely valuable as will guide the evacuation process based on user mobile phone location services.
2. The core of our solution is the efficient evacuation planning algorithm. An evacuation planning algorithm based on artificial potential field (APF) is proposed. The basic idea of APF is to establish a model of artificial potential field to describe the complex large-scale evacuation problem with the potential field function, which simplifies the difficulty of modelling the complex disaster scenario, and enhances the efficiency and accuracy.
3. In order to realize a more humanitarian evacuation, we take the interpersonal relationships into consideration, and propose an evacuation planning algorithm based on artificial potential field with relationship attractions (APF-RA). We introduce the relationship attraction potential field into the ultimate resultant potential field function. Under the premise of the safety, evacuees with relationships can be evacuated to the same shelter. Both APF and APF-RA are applied to our solution.

To describe our contributions, the rest of the paper has been organized as follows. Section 2 analyzes the related works in evacuation planning mechanisms and systems. Section 3 describes the architecture and the operation process of our system. Section 4 describes APF and APF-RA in detail. Then, Section 5 carries on the contrast experiments to the algorithms. The final section concludes the paper by summarizing the main contributions and points out the future research directions.

2 RELATED WORKS

X. Song et al. [1], [2] builds the model of the large-scale evacuation behaviors by constructing a large human mobility database, and then extract the characteristics of evacuation behaviors for individuals during the disasters. The evacuation behaviors of victims are modeled by the Markov decision process (MDPs), and then the parameters of the model are trained to find new migration characteristics. A general probabilistic model of evacuees under complicated geographical features is proposed. B. Tang et al. [3] presents a Robot-Assisted evacuation scheme, and E. Boukas et al. [4] presents an accurate Cellular Automaton simulation model, which are capable of assessing the human behavior and mobility during emergency situations. The setting of parameters of both proposed schemes need to be determined empirically, and there exists a contradiction between temporal and spatial overhead and the solution accuracy. In addition, both schemes do not consider the interactions between the evacuees and the dynamic distribution of the population. V.S. Kalogeiton et al. [5] takes inspiration from the slime mould behavior and propose a computational bio-inspired model crowd evacuation model, which mimicks the Physarum foraging process, the food diffusion, the organism's growth, the creation of tubes for each organism, the selection of optimum tube for each human in correspondence to the crowd evacuation and finally the movement of all humans at each time step towards near exits. However, the model is only designed and suitable for indoor environments. M. Di Gangi et al. [6] analyses a

In view of the above problems, the main contributions of this paper include:

1. Based on the IoT and mobile Cloud computing platform, we construct an evacuation planning system for large-scale evacuees. The system realizes the cooperation between mobile terminals and Cloud servers: mobile terminals submit the location information of evacuees and other collected information to Cloud servers; the Cloud server push the information of disaster to mobile terminals and then provide the personalized evacuation planning schemes for mobile terminals.

transportation system under emergency conditions and proposes a microscopic dynamic traffic assignment (DTA) model to determine quantitative indicators of traffic situation in the disaster area. In particular, a new version that is able to allow for multimodal networks and to consider network reliability is introduced. The method only solves the problem of the distribution of the evacuation road network and does not take the humanitarian factors into account. L. Chen et al. [7] proposes a load-balancing framework for distributed emergency guiding based on wireless sensor networks which can achieve the load balancing and reduce the total evacuation time. And an analytical model is derived, which can provide the fastest path for people to reach an exit according to the evacuation time estimated using the analytical model. However, the scheme is limited to indoor environments. P. Tsai et al. [8] presents a dynamic event-dependent network model. Rapid calculation and storage of the path becomes an important link in any emergency situation. The model can quickly calculate the evacuation direction of the evacuees to reach the nearest shelter. However, the model does not take the load balancing of shelters into account. In addition, the model does not take global evacuation planning into account. S. Mukherjee et al. [9] puts forward the Lagrangian approach to the modeling of crowd dynamics by considering the various forces that act between the members of a crowd while they are in motion, which is demonstrated via the Lyapunov energy function and the variable gradient method. But the model has not been applied to disaster scenarios.

M. U. S. Khan et al. [10] proposes a scalable emergency evacuation service, termed the MacroServ which recommends the evacuees with the most preferred routes towards safe locations in disaster scenes. The approach considers real-time road conditions to compute the maximum flow capacity of routes in the transportation network. The evacuees are directed towards those routes that are safe and have least congestion resulting in decreased evacuation time. However, the system need to extend by incorporating more number of parameters and the relevant factors of humanitarian evacuation to address the uncertain factors in emergency. Y. Iizuka et al. [11] presents a system that supports people being evacuated effectively from dangerous situations by using Multi-Agent cooperation. The system evaluates the location of evacuees by using mobile devices and performing distributed computing. A distributed constraint optimization problem (DCOP) is used to model and solve the evacuation problem. Finally, an experiment was carried out using multi-agent simulation. However, the formalization in this paper is very simple, it is necessary to introduce a more realistic model and take the problem of load balancing in shelters into consideration. P. G. Raj et al. [12] puts forward a distributed mobile sensing based crowd evacuation system and the multiple crowd guidance algorithm. The BigActors model is applied to the system, which can be used for evacuation guidance. But the system is also suitable for indoor environment and lacks of humanitarian consideration. K. M. Yu et al. [13] proposes an intelligent guidance system that is a combination of image

recognition and sigital signage for conducting people to safety. The system uses WSN and RFID to collect the environmental information, and uses smartphones and digital signages to guide people to the exit rapidly. However, the system is only used for indoor environment and needs to deploy digital signages, which brings the high hardware cost. F. Zhu et al. [14] presents a parallel public transportation system (PPTS) based on the artificial societies. PPTS was applied to the 2010 Guangzhou Asian Games, and the effectiveness of the is verified through the evaluation of two transportation evacuation plans for the Asian Games. But the system does not take the evacuation of people to the shelters into account and is lack of humanitarian consideration. O. Khalid et al. [15] presents an emergency evacuation system called EvacSys which is based on Cloud computing technology. The biggest problem in the evacuation process is the availability of effective information and through a safe route to evacuate from the affected areas. The Cloud-based EvacSys processes a large amount of real-time sensory data to compute safe and appropriate routes for evacuees and emergency vehicles in disaster situations. But the system does not take the psychological state of the evacuees and the problem of humanization evacuation into account.

3 IOT EVACUATION PLANNING SYSTEM

This section presents the generic architecture of the Crowd Lives Oriented Track and Help Optimization System (CLOTHO). CLOTHO a typical IoT based disaster management scenario, where evacuation of people is based on user mobile phones.

3.1 System Architecture

Based on the mobile Cloud computing platform, we con-

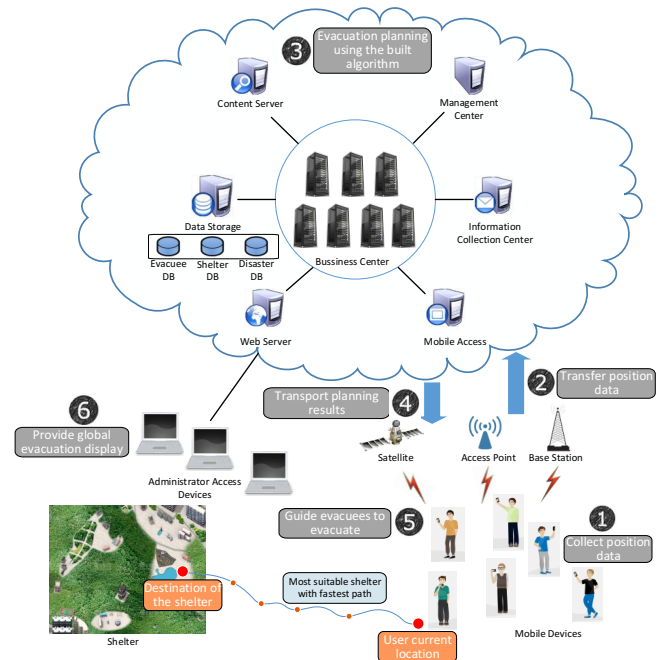


Fig. 1. The system architecture of CLOTHO

struct an efficient evacuation planning system for large-

scale crowd. Fig. 1 shows the CLOTHO architecture.

CLOTHO has four main modules, including the data acquisition, the network transmission, the Cloud service and the user access. The data acquisition module is mainly responsible for collecting the location information of the evacuees, including the latitude and the longitude, via mobile devices, such as smartphones. The network transmission module is responsible for two-way communications between mobile devices and Cloud servers based on the basic wireless communication network infrastructure. The Cloud service module is the core component of CLOTHO, which is based on the Cloud data center. The Cloud service module receives the data from the data acquisition module and provides services of data storage and data processing. The main tasks of the Cloud service module are managing the information of evacuees, shelters, and disasters and then providing personalized evacuation schemes for crowd in disaster.

The user access module is used as the interactive interface for users to obtain the evacuation services from the Cloud service module, including the browser-based access interface for the administrators of the emergency command center, and the visualized evacuation planning display interface for mobile terminals.

3.2 Typical Scenario

In this work, we consider as a typical disaster scenario the explosion of a chemical plant in Nanjing, China. When the disaster happened, toxic chemicals leaked and spreaded quickly. CLOTHO captured the time, location, affected area and other information of the disaster and pushed them to those mobile terminals held by users needing to be evacuated. CLOTHO has the locations of all users online and the surrounding shelters, as shown in Fig. 2(a). Then, based on the locations of users and shelters and other information (exp. the interpersonal relationships), CLOTHO used the built-in evacuation planning algorithm to provide the personalized evacuation planning schemes for users in order to guide them to the most reasonable shelters. Based on the user access module, users can see the visualized evacuation planning schemes on the screen of their smartphones with the routes, distances and time of evacuation, as shown in Fig. 2(b). The user can obtain the specific evacuation guidance. According to the real-time traffic condition, the system recommends the best personalized evacuation routes and avoids the congested roads actively, as shown in Fig. 2(c). In addition, the system provides the shelter information query function, as shown in Fig. 2(d).

In addition, CLOTHO can provide services for the emergency management agency. Fig. 3 shows the real-time evacuation situations, where each red mark indicates the location of each person to be evacuated, each black mark indicates the location of each shelter, and each blue line linking an evacuee and a shelter indicates a recommended evacuation direction. As shown in Fig. 3, more and more people in the area of the disaster have been evacuated to the shelters safely as time goes on.

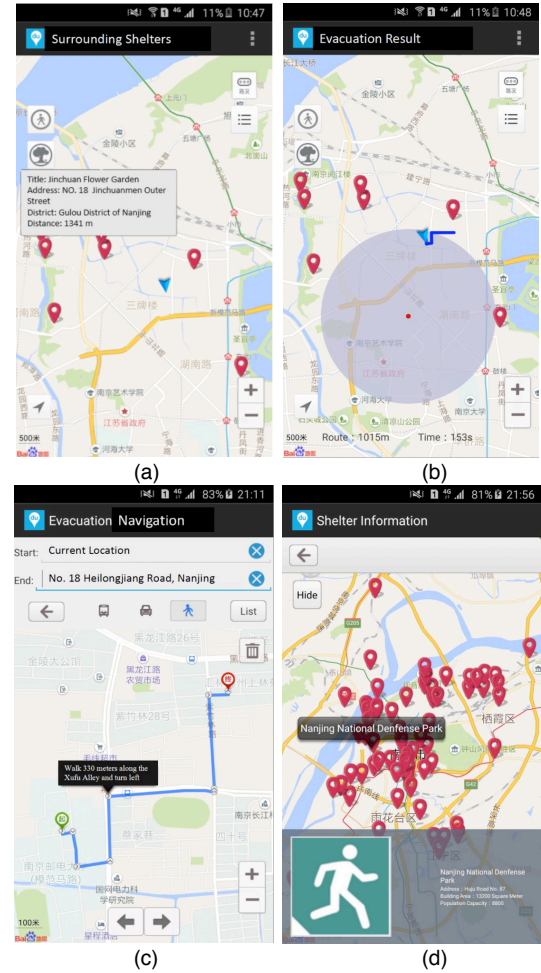


Fig. 2. The smartphone interface of CLOTHO. (a) Surrounding shelters (b) Route, distance and time of evacuation (c) Evacuation route recommendation. (d) Shelter information query.

As we mentioned above, the evacuation planning algorithm determines the performance of CLOTHO. In the following section, we will present two evacuation planning algorithms.

4 EVACUATION PLANNING ALGORITHM

4.1 Problem Analysis

The disaster emergency evacuation planning problem is an NP-hard problem [16] and includes different methods to solve it, based on the research results of physics, genetics and bionics have been proposed. These include Simulated Annealing (SA) [17], Tabu Search (TS) [18], Gravitational Search Algorithm (GSA) [19], Genetic Algorithm (GA) [20], [21], Ant Colony Optimization (ACO) [22], etc. However, there are some shortcomings of the emergency evacuation planning mechanisms based on heuristic algorithms, such as slow convergence, premature convergence and local optimization. Before presenting our evacuation planning algorithm, we need to make three reasonable assumptions.

tial field proposed in this paper, APF, is to make evacuees move towards the fastest decline directions of the total potential field with the gradient descent search method. The disaster point produces repulsion forces on evacuees. The shelters generate attraction forces on evacuees. The resultant forces of the attraction forces and the repulsion forces control the moving of evacuees. As shown in Figure 5, the closer to the shelters, the smaller the potential field value; the closer to the disaster point, the greater the potential field value [24].

The theory of artificial potential field points out that in any environmental space, as long as there is a target point can produce a calculatable artificial potential field [23]. The forces on an evacuee X_j in the potential field are shown in Fig. 6.

Definition 1. Total Potential Field. In an emergency scenario, an evacuee is considered in a configuration space as a particle subjected to an artificial potential field called the total po-

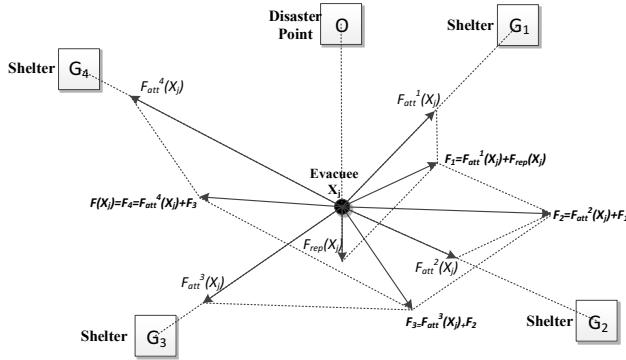


Fig. 6. The forces on an evacuee based on the artificial potential field.

tential field.

Definition 2. Attraction Potential Field. The attraction potential field is used to describe the force of attraction generated by the shelters in a configuration space.

Definition 3. Repulsion Potential Field. The repulsion potential field is used to describe the force of repulsion generated by the disaster point in a configuration space.

Supposing that the collection of the shelters is $G=(G_1, G_2, \dots, G_i, \dots, G_m)$, the collection of the evacuees is $X=(X_1, X_2, \dots, X_j, \dots, X_n)$ the coordinates of an evacuee is $X_j=(x_j, y_j)$, and the coordinates of the shelter i is $G_i=(x_i, y_i)$, the total potential field function $U(X_j)$ can be defined as

$$U(X_j) = \sum_{i=1}^m U_{att}^i(X_j) + U_{rep}(X_j) \quad (1)$$

where $U_{att}^i(X_j)$ represents the attraction potential field generated by the shelter G_i , and $U_{rep}(X_j)$ represents the repulsion potential field generated by the point $O=(x_o, y_o)$ where the disaster happens.

We define the attraction potential field generated by the shelter G_i as

$$U_{att}^i(X_j) = \frac{1}{2} k \cdot \rho(X_j, G_i)^2 \quad (2)$$

where k is the attraction coefficient, and $\rho(X_j, G_i)$ is the Euclidean distance from X_j to G_i . The Euclidean distance between $X_j=(x_j, y_j)$ and $G_i=(x_i, y_i)$ is defined as

$$\rho(X_j, G_i) = 2 \cdot R_e \cdot \arcsin\left(\sqrt{\sin^2\left(\frac{a}{2}\right) + \cos(y_j) \times \cos(y_i) \times \sin^2\left(\frac{b}{2}\right)}\right) \quad (3)$$

where $a=|y_j - y_i|$ is the difference between the latitudes of X_j and G_i , $b=|x_j - x_i|$ is the difference between the longitudes of X_j and G_i , and $R_e=6378.137$ represents the spherical radius of the earth.

We use the FIRAS function [24] to establish the repulsion potential field function

$$U_{rep}(X_j) = \frac{1}{2} m \left(\frac{1}{\rho(X_j, O)} - \frac{1}{\rho_0} \right)^2 \quad (4)$$

where m is the repulsion coefficient, $\rho(X_j, O)$ denotes the Euclidean distance from X_j to O , and ρ_0 represents the radius of the repulsion potential field, i.e. the effect area of the disaster.

Definition 4. Virtual Resultant force. The virtual resultant force is the total force that is subjected to the moving direction of the evacuee.

Definition 5. Attraction Force. The attraction force shows the attraction effect of the shelters to the evacuee in a configuration space.

Definition 6. Repulsion Force. The repulsion force shows the repulsion effect of the disaster point to the evacuee in a configuration space.

The virtual force on evacuee is defined as the negative gradient of the potential field. Therefore, the virtual resultant force $F(X_j)$ is defined as

$$F(X_j) = -\nabla U(X) = \sum_{i=1}^m F_{att}^i(X_j) + F_{rep}(X_j) \quad (5)$$

where $F_{att}^i(X_j)$ represents the attraction force from G_i , and $F_{rep}(X_j)$ represents the repulsion force from O .

The attraction force from G_i on the evacuee is defined as

$$F_{att}^i(X_j) = -\nabla(U_{att}^i(X_j)) = -k \cdot \rho(X_j, G_i) \quad (6)$$

where $F_{att}^i(X_j)$ is a vector pointing to X_j , and the strength of $F_{att}^i(X_j)$ is associated with X_j and G_i .

The repulsion force is defined as the negative gradient of the repulsion potential field

$$\begin{aligned} F_{rep}(X_j) &= -\nabla(U_{rep}(X_j)) \\ &= m \left(\frac{1}{\rho(X_j, O)} - \frac{1}{\rho_0} \right) \cdot \frac{1}{\rho^2(X_j, O)} \cdot \nabla \rho(X_j, O) \end{aligned} \quad (7)$$

where $\nabla \rho(X_j, O)$ represents a unit vector from O pointing to X_j .

Definition 7. Shelter Distance Threshold. The shelter distance threshold ρ_G is a constant. The attraction potential field generated by the shelters can be controlled by ρ_G , so as to eliminate the adverse effects of the shelters on the evacuees.

Definition 8. Disaster Distance Threshold. The disaster distance threshold ρ_o is a constant. The repulsion potential field generated by the disaster point can be controlled by ρ_o .

The workflow of APF is shown in Fig. 7:

Step 1. The rectangular coordinate system xoy is established by the longitude x_j and latitude y_j of X_j . Suppose that the angle between the link from the coordinates of the evacuee X_j to the shelter $G_i=(x_i, y_i)$ (identified as $\rho(X_j, G_i)$) and the x-axis is α_{ij} , the angle between the link from the coordinates of the evacuee X_j to the disaster point (identified as $\rho(X_j, O)$) and the x-axis is β_j , and the angle of the

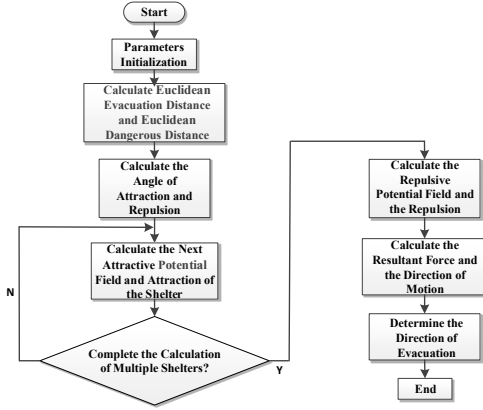


Fig. 7. The workflow of the evacuation planning algorithm based on artificial potential field.

virtual resultant force and the x-axis is η_j . The initialization operations are performed on α_{ij} , β_j , η_j , n , ρ_o and ρ_G .

Step 2. According to the evacuee's coordinate $X_j=(x_j, y_j)$ and the disaster point's coordinate $O=(x_o, y_o)$, the distance between the evacuee and the disaster point, d_{oj} , called the Euclidean dangerous distance, is calculated and obtained with (3). According to $X_j=(x_j, y_j)$ and the shelters' coordinate $G_i=(x_i, y_i)$, the distance between the evacuee X_j and the shelters, d_{Gj} , called the Euclidean evacuation distance, is also calculated and obtained with (3).

Step 3. Each candidate shelter (G_i) is determined whether it satisfies $d_{Gj} \leq \rho_G$ or not. The suitable shelters are labeled as the available shelters.

Step 4. α_{ij} and β_j are calculated with the inverse trigonometric function

$$\alpha_{ij} = \begin{cases} \arcsin \frac{x_i - x_j}{\rho(X_j, G_i)}, x_i - x_j > 0, y_i - y_j > 0 \\ \pi - \arcsin \frac{x_i - x_j}{\rho(X_j, G_i)}, x_i - x_j < 0, y_i - y_j > 0 \\ \pi + \arcsin \frac{x_i - x_j}{\rho(X_j, G_i)}, x_i - x_j < 0, y_i - y_j < 0 \\ \frac{3}{2}\pi + \arcsin \frac{x_i - x_j}{\rho(X_j, G_i)}, x_i - x_j > 0, y_i - y_j < 0 \end{cases} \quad (8)$$

$$\beta_j = \begin{cases} \arcsin \frac{x_o - x_j}{\rho(X_j, X_o)}, x_o - x_j > 0, y_o - y_j > 0 \\ \pi - \arcsin \frac{x_o - x_j}{\rho(X_j, X_o)}, x_o - x_j < 0, y_o - y_j > 0 \\ \pi + \arcsin \frac{x_o - x_j}{\rho(X_j, X_o)}, x_o - x_j < 0, y_o - y_j < 0 \\ \frac{3}{2}\pi + \arcsin \frac{x_o - x_j}{\rho(X_j, X_o)}, x_o - x_j > 0, y_o - y_j < 0 \end{cases} \quad (9)$$

Step 5. $U_{att}^i(X_j)$ and $F_{att}^i(X_j)$ from each shelter G_i are calculated with (2) and (6) respectively.

Step 6. $U_{rep}(x_j)$ and $F_{rep}(x_j)$ from the disaster point O are calculated with (4) and (7) respectively.

Step 7. The orthogonal decomposition method of force calculation is adopted. According to α_{ij} and β_j , the sum of

forces in the x-axis F_{sumx} and in the y-axis F_{sumy} can be calculated respectively. Assume the point $D=(F_{sumx}, F_{sumy})$, the total potential field $U(X_j)$ and the virtual resultant force

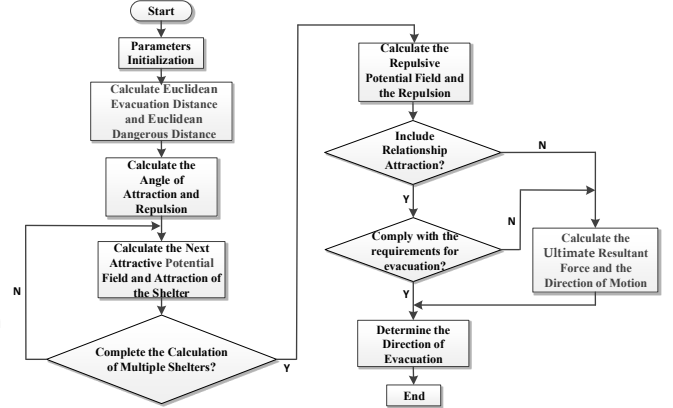


Fig. 9. Flow chart of Evacuation planning algorithm based on artificial potential field with relationship attraction.

$F(X_j)$ are calculated with (1) and (5), and then η_j is calculated with

$$\eta_j = \begin{cases} \arcsin \frac{F_{sumx} - x_j}{\rho(X_j, D)}, F_{sumx} - x_j > 0, F_{sumy} - y_j > 0 \\ \pi - \arcsin \frac{F_{sumx} - x_j}{\rho(X_j, D)}, F_{sumx} - x_j < 0, F_{sumy} - y_j > 0 \\ \pi + \arcsin \frac{F_{sumx} - x_j}{\rho(X_j, D)}, F_{sumx} - x_j < 0, F_{sumy} - y_j < 0 \\ \frac{3}{2}\pi + \arcsin \frac{F_{sumx} - x_j}{\rho(X_j, D)}, F_{sumx} - x_j > 0, F_{sumy} - y_j < 0 \end{cases} \quad (10)$$

Step 8. The evacuation direction of the evacuee X_j is determined with the resultant force $F(X_j)$ and resultant force angle η_j . Find the minimum value of $|\eta_j - \alpha_{ij}|$, that is to determine the deviation of the shelter G_i and evacuation angle η_j is the smallest, and finally the shelter G_i is used as the evacuation destination.

Step 9. The algorithm ends.

4.3 Relationship Attraction Force

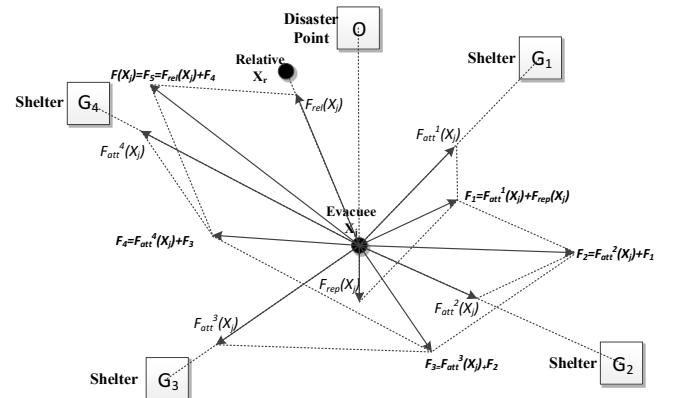


Fig. 8. The forces on an evacuee based on the artificial potential field with relationship attraction.

The efficient evacuation must consider the mentality, emotion and behavior of people [25]. Therefore, it is obvious that evacuating people with relationships to the same shelter will ease their nervous or fear moods effectively, so as to achieve the more humanitarian evacuation. With relationships, we improve APF to APF-RA. The forces on an evacuee X_j in the potential field with relationship attraction are shown in Fig. 8.

Definition 9. Relationship Attraction Potential Field. The attraction potential field is used to describe the force of attraction generated by the relationship of the evacuee in a configuration space.

Definition 10. Relationship Attraction Force. The relationship attraction force shows the attraction effect of the relationship of the evacuee in a configuration space.

The relationship attraction potential field is introduced into the total potential field function. The total potential field with relationship attraction can be expressed as:

$$U(X_j) = \sum_{i=1}^m U_{att}^i(X_j) + U_{rep}(X_j) + U_{rel}(X_j) \quad (11)$$

where $U_{rel}(X_j)$ is the relationship attraction potential field. It is defined as

$$U_{rel}(X_j) = \begin{cases} \frac{1}{2}b \cdot \rho(X_j, X_r)^2, & \rho(X_j, X_r) \leq \rho_e \\ 0, & \rho(X_j, X_r) > \rho_e \end{cases} \quad (12)$$

where b is the relationship attraction coefficient, $\rho(X_j, X_r)$ is the Euclidean distance between the evacuee X_j and his/her relative X_r , and ρ_e is the action distance of the relationship attraction potential field.

The virtual resultant force with the relationship attraction force can be simplified to:

$$F(X_j) = \sum_{i=1}^m F_{att}^i(X_j) + F_{rep}(X_j) + F_{rel}(X_j) \quad (13)$$

where $F_{rel}(X)$ is the relationship attraction force. It is defined as the negative gradient of the relationship attraction potential field

$$F_{rel}(X_j) = -\nabla(U_{rel}(X_j)) = \begin{cases} -b \cdot \rho(X_j, X_r), & \rho(X_j, X_r) \leq \rho_e \\ 0, & \rho(X_j, X_r) > \rho_e \end{cases} \quad (14)$$

Definition 11. Relationship Attraction Distance Threshold. The relationship attraction distance threshold ρ_e is a constant. The attraction potential field generated by the relative can be controlled by ρ_e , so as to eliminate the adverse effects of the relationship on the evacuees.

The rectangular coordinate system xoy is established by the longitude x_j and latitude y_j of X_j . The angle between the link from the coordinates of X_j to the shelter $G_i=(x_i, y_i)$ (identified as $\rho(X_j, G_i)$) and the x-axis is α_{ij} , the angle between the link from the coordinates of X_j to the disaster point (identified as $\rho(X_j, O)$) and the x-axis is β_j , and the angle between the link from the coordinates of X_j to X_r (identified as $\rho(X_j, X_r)$) and the x-axis is σ_j . The angle between the virtual resultant force (included attraction force

and repulsion force) and the x-axis is η_j^1 , and the angle between the virtual resultant force with the relationship attraction force (included attraction force, repulsion force and relationship attraction force) and the x-axis is η_2 .

The process of APF-RA is shown in Fig. 9:

Step 1. The initialization operations are performed with $\alpha_{ij}, \beta_j, \eta_j^1, \sigma_j, \eta_j^2, n, \rho_0, \rho_G$ and ρ_e .

Step 2. According to the evacuee's coordinate $X_j=(x_j, y_j)$ and the disaster point's coordinate $O=(x_0, y_0)$, the distance between the evacuee and the disaster point, d_0 , called the Euclidean distance of dangerous, is calculated with (3). According to $X_j=(x_j, y_j)$ and his/her relative's coordinate $X_r=(x_r, y_r)$, the distance between the evacuee X_j and X_r , d_r , called the Euclidean relationship distance, is also calculated and obtained with (3).

Step 3. Each candidate shelter (G_i) is determined whether it satisfies $d_{Gi} \leq \rho_G$ or not. The suitable shelters are labeled as the available shelters.

Step 4. α_{ij} and β_j are calculated with (8) and (9).

Step 5. $U_{att}^i(X_j)$ and $F_{att}^i(X_j)$ from each shelter are calculated with (2) and (6) respectively.

Step 6. $U_{rep}(x_j)$ and $F_{rep}(x_j)$ from O are calculated with (4) and (7) respectively.

Step 7. The orthogonal decomposition method of force calculation is adopted. According to α_{ij} and β_j , the resultant forces (included attraction force and repulsion force) in the x-axis F_{sumx} and in the y-axis F_{sumy} are calculated respectively. Assume $D^1=(F_{sumx}, F_{sumy})$ as a point of the rectangular coordinate system xoy , $U(X_j)$ and $F(X_j)$ are calculated with (1) and (5), and then η_j^1 is calculated with (10).

Step 8. Determine whether there is relationship attraction. If so, $U_{rel}(x_j)$ and $F_{rel}(x_j)$ from O are calculated with (12) and (14) respectively, and then go to Step 9. Otherwise, turn to Step 12.

Step 9. Determined whether it satisfies $d_r \leq \rho_e$ or not. If so, continue to Step 10. Otherwise, turn to Step 12.

Step 10. The orthogonal decomposition method of force calculation is adopted. According to α_{ij}, β_j and σ_j , the sum of forces (included attraction force, repulsion force, relationship attraction force) in the x-axis is F_{sumx} and in the y-axis is F_{sumy} can be calculated respectively. Assume $D^2=(F_{sumx}, F_{sumy})$ as a point of as a point of the rectangular coordinate system xoy , $U(X_j)$ and $F(X_j)$ are calculated further with (11) and (13), and then η_j^2 is calculated with (10). Determine whether $\varepsilon=|\sigma_j - \eta_j^2|$ (i.e. the angle between the virtual resultant force and relationship attraction force) is satisfied the evacuation condition. If so, continue to Step 11. Otherwise, turn to Step 12.

Step 11. The evacuation direction of the evacuee X_j is determined with the relationship attraction angle σ (i.e. the shelter where X_r is located as the evacuation destination of X_j) so as to bring evacuees the the same shelter.

Step 12. The evacuation direction of X_j is determined with $F(X_j)$ and η_j^1 . Find the minimum value of $|\eta_j^1 - \alpha_{ij}|$, that is to determine the deviation of the shelter and evacuation angle η_j^1 is the smallest, and finally the shelter is determined as the evacuation destination.

Step 13. The algorithm ends.

5 EXPERIMENTS

5.1 Experimental Scenario

We used a typical disaster event happened in Nanjing, China, as shown in Fig. 10. The specific coordinate of the disaster is (118.774388°E, 32.07471°N). The radius of the effect area of the disaster is 1.6 km, which affects 8.042 square kilometers.

There are 12 shelters within the radius of 2.5 km totally. As shown in Table 1, these shelters can contain 139,833 persons totally.

Assume that the total number of evacuees is 100, 200, 400, 800, 1500 and 2500 respectively. We designed and implemented a series of experiments to verify the effectiveness and convergence of APF and APF-RA algorithm, and compared their performances with typical algorithms, SA, TS and GSA respectively.

The capacity of shelter is adjusted proportionately, including the following two conditions:

1. Insufficient capacity. The total capacity of the shelters is 10% less than the number of people needing to be evacuated.
2. Sufficient capacity. The total capacity of the shelters is 10% more than the number of people needing to be evacuated.

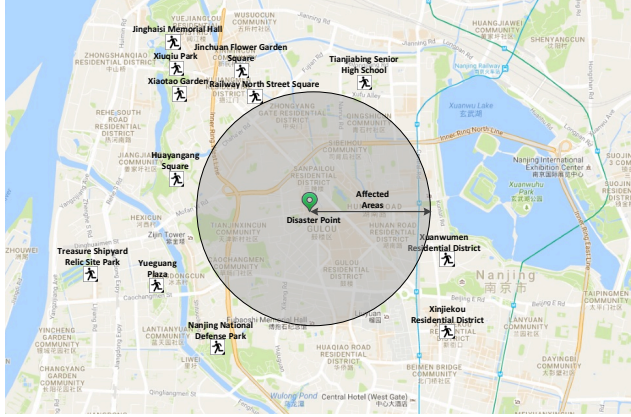


Fig. 10. The experimental scenario.

The parameters of these related algorithms are shown in Table 2.

To APF-RA, the relationship attraction coefficient b , the

TABLE 1
DATA OF THE SHELTERS

| ID | Title | Latitude and longitude | Construction area(m ²) | Capacity(people) |
|------------|-----------------------------------|------------------------|------------------------------------|------------------|
| 1657560983 | Nanjing National Defense Park | 118.761159, 32.057838 | 13200 | 8800 |
| 1657561005 | Xuanwumen Residential District | 118.793484, 32.071386 | 5000 | 3333 |
| 1657561011 | Xinjiakou Residential District | 118.795624, 32.059467 | 8000 | 5333 |
| 1657561055 | Treasure Shipyard Relic Site Park | 118.742962, 32.067632 | 50000 | 33333 |
| 1657561059 | Yueguang Plaza | 118.75146, 32.065886 | 10000 | 6666 |
| 1657561060 | Tianjia Senior High School | 118.783814, 32.090255 | 15000 | 10000 |
| 1657561062 | Railway North Street Square | 118.765426, 32.09196 | 10000 | 6666 |
| 1657561063 | Xinqiu Park | 118.752392, 32.095057 | 59555 | 39703 |
| 1657561064 | Jinhua Memorial Hall | 118.751757, 32.097245 | 15000 | 10000 |
| 1657561066 | Xiatiao Garden | 118.753183, 32.092113 | 20000 | 13333 |
| 1657561073 | Jinchuan Flower Garden | 118.764747, 32.094514 | 2000 | 1333 |
| 1657561075 | Huayangang Square | 118.755086, 32.080763 | 2000 | 1333 |

ultimate resultant force angle η_2 and the relationship attraction angle ε are set according to the degree of relationship, as shown in Table 3.

5.2 Experimental Results and Performance analysis

Experiment 1. Route and time of evacuation.

In Fig. 11, the evacuation routes with different algorithms are compared in two cases of sufficient capacity and insufficient capacity respectively. It can be seen from Fig. 11 that the evacuation routes of these algorithms in case of sufficient capacity are shorter than in case of insufficient capacity. In case of insufficient capacity, it can only be considered to evacuate to further shelter. This will lead to an increase to the evacuation routes inevitably.

In general, the evacuation route of SA and GSA is the longest. Due to the "premature" defect of them, they tend to output an obtained local optimal solution as the global

TABLE 2
PARAMETERS OF ALGORITHMS

| Algorithm | Parameter | Value |
|-----------|---|-------|
| SA | Temperature initialization | 5 |
| | Lower bound of temperature T_{min} | 1.2 |
| | Temperature drop rate | 0.96 |
| | The number of iterations value k | 3 |
| TS | Shelter distance Threshold ρ_{ts} | 2500 |
| | The number of iterations value G_{max} | 10 |
| | Tabu length L_{tabu} | 3 |
| GSA | Shelter distance threshold ρ_{ts} | 2500 |
| | Attraction coefficient G_0 | 100 |
| APF | Shelter distance threshold ρ_{ts} | 2500 |
| | Disaster distance threshold ρ_{ds} | 1600 |
| APF-RA | Shelter distance threshold ρ_{ts} | 2500 |
| | Disaster distance threshold ρ_{ds} | 1600 |
| | Relationship attraction distance threshold ρ_r | 3000 |

optimal solution. Secondly is TS, it accepts parts of the poor solutions by creating a tabu list, which will lead to output some local optimal solutions as global optimal solutions. The evacuation route of APF and APF-RA is the shortest. By introducing the disaster distance threshold ρ_{or} ,

TABLE 3
PARAMETERS RELATED TO RELATIONSHIPS

| Level | Classification | Relationship attraction coefficient b | The virtual resultant force and relationship attraction force angle ε |
|-------|-------------------------------------|---|---|
| 1 | Parents, children, husband and wife | 1 | $0^\circ \leq \varepsilon < 90^\circ$ |
| 2 | Relative | 0.8 | $0^\circ \leq \varepsilon < 60^\circ$ |
| 3 | Friends, classmates | 0.6 | $0^\circ \leq \varepsilon < 30^\circ$ |

the range of the repulsion potential field can be adjusted and the local minimum problem of the algorithms are improved.

Because SA, TS and GSA are easy to fall into the local optimum, the capacity allocation of the shelter is unbalanced. In the later period, they only consider the further shelters in the evacuation planning process, so the length of evacuation routes will be greatly increased with the increase of evacuee. APF and APF-RA establish the potential field in the disaster environment, they maintain the balance of shelter allocation during the evacuation process, so the evacuation route length tends to be stable as the size of the evacuees expands.

Fig. 12 shows the evacuation time with different algorithms are compared in two cases of sufficient capacity and insufficient capacity. It can be seen from Fig. 12 that the evacuation time of these algorithms in case of sufficient capacity are shorter than in case of insufficient capacity. In case of insufficient capacity, it can only considered to evacuate to further shelter. This will lead to an increase to the evacuation time inevitably.

In Fig. 12(a), the descending order of the evacuation time is GSA, SA, TS, APF and APF-RA. Because SA, TS and GSA are easy to fall into the local optimum, the capacity allocation of the shelter is unbalanced and the evacuation time is longer. APF and APF-RA establish the potential field in the disaster environment, and maintain the balance of the shelter allocation during the evacuation process. With the increase of evacuees, the overall evacuation time is shorter.

In Fig. 12(b), when the number of evacuee is 200, the evacuation time of SA and TS is the shortest. The reason is that APF and APF-RA describe the disaster environment with the potential field function and take real-time residual capacity parameter of the shelters as the attraction coefficient, so that the capacity of the shelter in the evacuation process is balanced, which saves a lot of evacuation time. In the evacuation of fewer evacuees, this advantage can not be fully reflected. However, the advantages of APF and APF-RA are more and more obvious with the increase of evacuees.

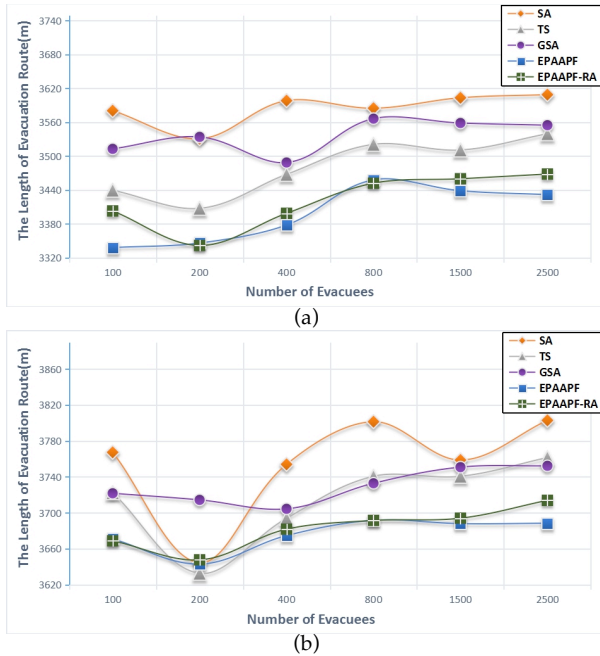


Fig. 11. The average length of evacuation route. (a)Under the condition of capacity remaining. (b)Under the condition of insufficient capacity.

Experiment 2. Evacuation success rate.

In Fig. 13, the evacuation success rate with different algorithms are compared in two cases of sufficient capacity

and insufficient capacity respectively. It can be seen from Fig. 13 that the evacuation success rate of these algorithms in case of sufficient capacity is higher than in case of insufficient capacity. In case of insufficient capacity, the capacity allocation of the shelter is more difficult, the number of the evacuees failed to evacuate increases, so the overall evacuation success rate is low.

In Fig. 13(a), SA, TS and GSA are easy to fall into the local optimum, the capacity allocation of the shelter is unbalanced, and the evacuation success rate is low. APF and APF-RA establish the potential field in the disaster environment, they maintain the balance of shelter allocation during the evacuation process, so the evacuation success rate is high. The advantages of APF and APF-RA are more and more obvious with the increase of evacuees. In Fig. 13(b), the evacuation success rate of GSA, APF and APF-RA is higher and remain stable gradually.

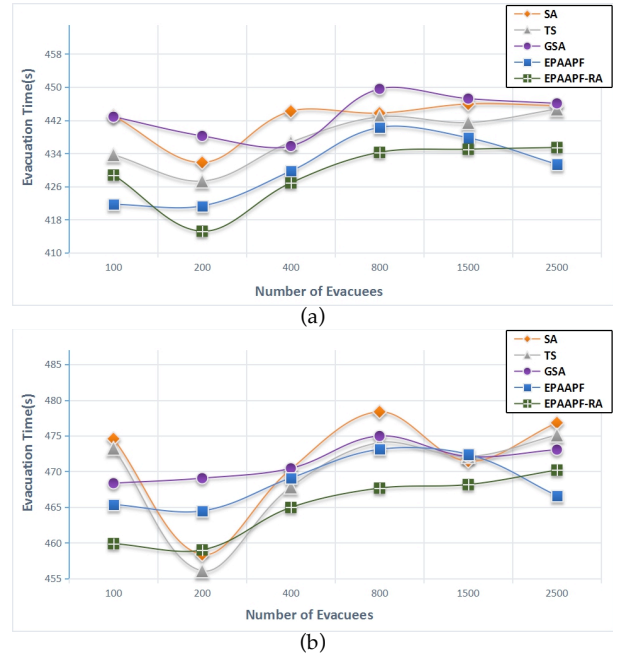


Fig. 12. The average evacuation time. (a)Under the condition of capacity remaining. (b)Under the condition of insufficient capacity.

Experiment 3. Evacuation efficiency of SA, TS, GSA, APF and APF-RA.

In Fig. 14, when the number of evacuee is 400, the evacuation efficiency are compared in two cases of suffi-

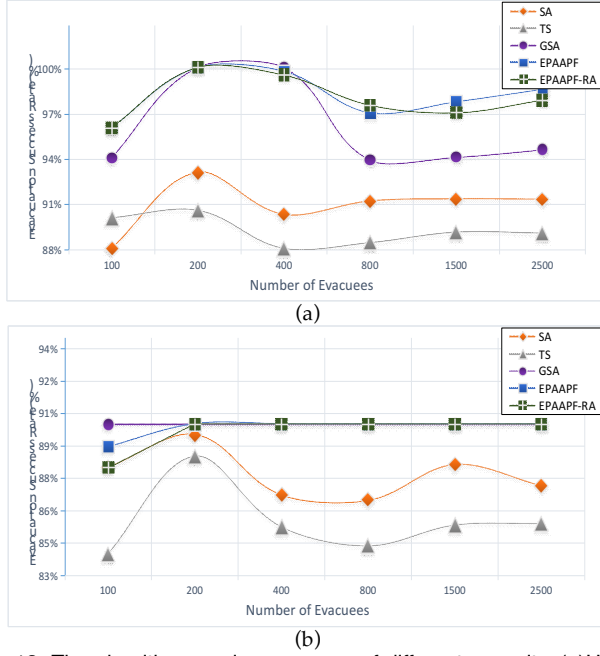


Fig. 13. The algorithm running accuracy of different capacity. (a) Under the condition of capacity remaining. (b) Under the condition of insufficient capacity.

cient capacity and insufficient capacity respectively. It can be seen that the evacuation efficiency of these algorithms in case of sufficient capacity is higher than in case of insufficient capacity. In the case of insufficient capacity, the capacity allocation of the shelter is more difficult, the number of the evacuees failed to evacuate increases, so the evacuation efficiency is low.

Fig. 14(a) reflects the evacuation efficiency curve in the case of insufficient capacity. It can be seen that the evacuation efficiency of SA and TS is low. In the early period, the evacuation percentage of GSA increases slowly. In general, APF and APF-RA show a rapid and steady increase of the evacuation percentage, which reflect their excellent performance.

Fig. 14(b) reflects the evacuation efficiency curve in the case of sufficient capacity. It can be seen that the evacuation efficiency of SA and TS is low. In the early period, the evacuation percentage of GSA increases fastly. In general, the evacuation efficiency of APF and APF-RA is the most ideal.

Experiment 4. Humanitarian evacuation verification.

In the experiment, the proportion of evacuees who have relatives to be evacuated is 20%. The two curves in Fig. 15 indicate the proportion of humanitarian evacuation success in case of sufficient capacity and insufficient capacity. It can be seen from Fig. 15 that the proportion of humanitarian evacuation success is higher in case of sufficient capacity. In case of insufficient capacity, the proportion of humanitarian evacuation success is lower.

The reason is that the capacity of the shelter is limited, in the case of insufficient capacity, some of the evacuees due to capacity problems can not evacuate to the same shelter with their relatives. Therefore, the capacity of the

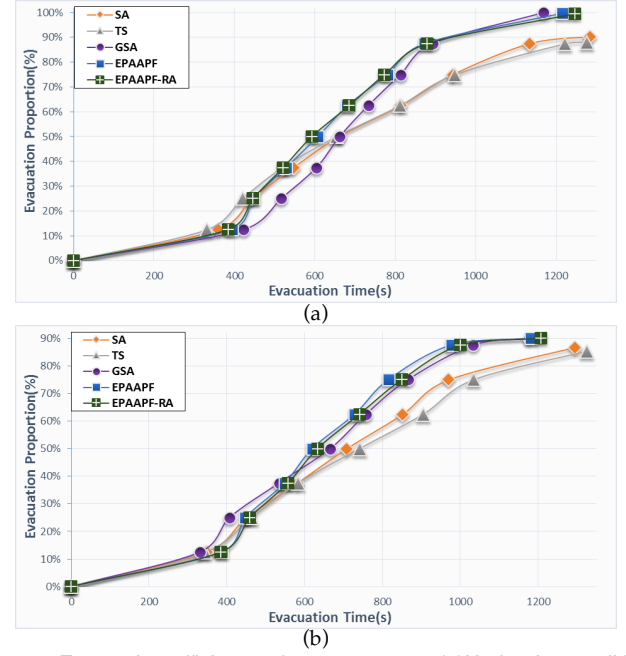


Fig. 14. Evacuation efficiency of 400 evacuees. (a) Under the condition of capacity remaining. (b) Under the condition of insufficient capacity.

shelter is more, the proportion of humanitarian evacuation success is higher.

Experiment 5. Computational complexity.

In Fig. 16, the time cost is compared in two cases from sufficient capacity and insufficient capacity respectively. It can be seen that the time cost of these algorithms in case of sufficient capacity is smaller than in case of insufficient capacity. In the case of insufficient capacity, it needs to

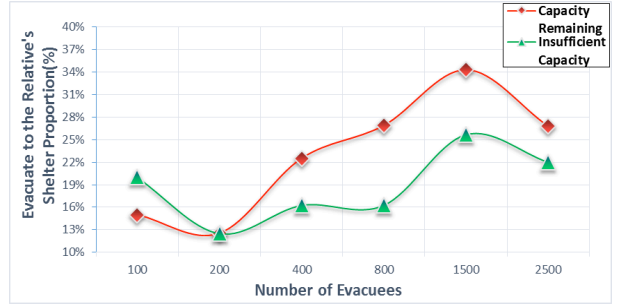


Fig. 15. Humanitarian evacuation proportion of different capacity.

operate several times in order to find a suitable shelter, the number of operations of the algorithm increases and results in the time cost increases.

In general, the computation cost is increased in the latter period of the searching process and resulted in a larger time cost of SA and TS due to the unbalance of shelter allocation. Secondly is TS, the length of the tabu list is too long that leads to an increase of the algorithm storage, so the time cost increases. APF and APF-RA establish the potential field in the disaster environment, and maintain the balance of the shelter allocation during the evacuation process, so the time cost is small.

In Fig. 14(b), the time cost of GSA is between APF and APF-RA when the number of evacuee is between 200 and 1500 people. The reason is that APF has the characteristics of small computational amount and high real-time, so the time cost is lower than other algorithms. APF-RA adds the judgment and calculation of relationship attraction

based on APF. This leads to a slightly higher time cost than APF. The time complexities of these algorithms are shown in Table 4. It can be seen from the table that the time complexity of TS and SA is larger, so the time cost of the two is higher. The time complexity of GSA, APF and APF-RA are smaller, so the time cost are lower. APF-RA adds the judgment and calculation of relationship attraction based on APF, but this does not cause an increase in the time complexity, so the performance of APF is guaranteed.

6 CONCLUSIONS

After the occurrence of large-scale disasters, rapid and orderly evacuation is very important. Orderly evacuation will largely ease the nervous and fear moods of the evacuees which is crucial to speed up the evacuation efficiency. Unfortunately, the existing evacuation algorithms only consider some aspects of the emergency evacuation planning problem.

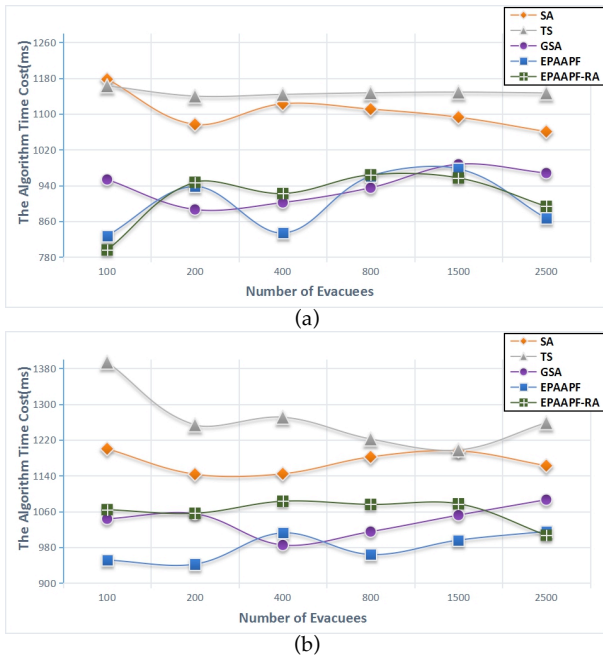


Fig. 16. Time cost of different capacity. (a) Under the condition of capacity remaining. (b) Under the condition of insufficient capacity.

TABLE 4
TIME COMPLEXITY ANALYSIS OF THE ALGORITHMS

| Algorithm | Time complexity |
|-----------|-----------------------|
| SA | $O(n \cdot \log_2 n)$ |
| TS | $O(n^2)$ |
| GSA | $O(n)$ |
| APF | $O(n)$ |
| APF-RA | $O(n)$ |

In this work, we propose an IoT based solution that can improve the accuracy and convergence speed while taking the load balance of the shelters into account. The contributions of this works include the following. Firstly, the APF-RA can ensure the evacuation of high efficiency with special attention to human psychological factors. What matters is that it can ease the anxiety, depression,

disturbance of consciousness and other psychological symptoms of evacuees which appear after the disaster occurs. Secondly, it realizes a more humanitarian evacuation. We apply APF and APF-RA to CLOTHO, which can effectively shorten the evacuation route length and evacuation time. They maintain the balance of the shelter allocation and achieve high efficiency and humanitarian evacuation. In addition, CLOTHO is currently available for emergency evacuation planning in a wide range of areas. However, the system has the potential to be extended to the indoor environment.

Future extensions of this work will aim to solve the following problems. Firstly, the dynamic evacuation planning problem, as the proposed algorithm performs well in a static system, but we aim to extend it in a dynamic system. Secondly, the evacuation route planning problem as the algorithm focus on planning for large-scale evacuees, so that the capacity of the surrounding shelters can be balanced, and the saturation problem of shelters can be avoided in the evacuation process. However, in future we will aim to solve the evacuation route planning problem.

References

- [1] X. Song, Q. Zhang, Y. Sekimoto, T. Horanont, S. Ueyama and R. Shibasaki, "Intelligent System for Human Behavior Analysis and Reasoning Following Large-Scale Disasters," *IEEE Intelligent Systems*, vol. 28, no. 4, pp. 35-42, Aug. 2013.
- [2] X. Song, Q. Zhang, Y. Sekimoto, T. Horanont, S. Ueyama and R. Shibasaki, "Modeling and probabilistic reasoning of population evacuation during large-scale disaster," in *Proc. 19th Acm Sigkdd Int. Conf. Knowledge Discovery And Data Mining*, 2014, pp. 1231-1239.
- [3] B. Tang, C. Jiang, H. He and Y. Guo, "Human Mobility Modeling for Robot-Assisted Evacuation in Complex Indoor Environments," *IEEE Trans. Human-Machine Systems*, vol. 46, no. 5, pp. 694-707, Oct. 2016.
- [4] E. Boukas, I. Kostavelis, A. Gasteratos and G. C. Sirakoulis, "Robot Guided Crowd Evacuation," *IEEE Trans. Automation Science and Engineering*, vol. 12, no. 2, pp. 739-751, April 2015.
- [5] V.S. Kalogeiton, D.P. Papadopoulos, I.P. Georgilas, G.C. Sirakoulis and A.I. Adamatzky, "Cellular automaton model of crowd evacuation inspired by slime mould," *International Journal of General Systems*, vol. 44, no. 3, pp. 354-391, Apr. 2015.
- [6] M. Di Gangi, "Modeling Evacuation of a Transport System: Application of a Multimodal Mesoscopic Dynamic Traffic Assignment Model," *IEEE Trans. on Intelligent Transportation Systems*, vol. 12, no. 4, pp. 1157-1166, Dec. 2011.
- [7] L. W. Chen, J. H. Cheng and Y. C. Tseng, "Distributed Emergency Guiding with Evacuation Time Optimization Based on Wireless Sensor Networks," *IEEE Trans. on Parallel and Distributed Systems*, vol. 27, no. 2, pp. 419-427, Feb. 1 2016.
- [8] P. H. Tsai, C. L. Lin and J. N. Liu, "On-the-Fly Nearest-Shelter Computation in Event-Dependent Spatial Networks in Disasters," *IEEE Trans. on Vehicular Technology*, vol. 65, no. 3, pp. 1109-1120, March 2016.
- [9] S. Mukherjee, D. Goswami and S. Chatterjee, "A Lagrangian Approach to Modeling and Analysis of a Crowd Dynamics," *IEEE Trans. on Systems, Man, and Cybernetics: Systems*, vol. 45, no. 6, pp. 865-876, June 2015.
- [10] M. U. S. Khan, O. Khalid, Y. Huang, R. Ranjan, F. Zhang, J. Cao,

- B. Veeravalli, S. Khan, K. Li and A. Zomaya, "MacroServ: A Route Recommendation Service for Large-Scale Evacuations," *IEEE Trans. on Services Computing*, vol. PP, no. 99, pp. 1-1, Nov. 2015
- [11] Y. Iizuka and K. Iizuka, "Disaster Evacuation Assistance System Based on Multi-agent Cooperation," in *Proc. 48th HICSS*, 2015, pp. 173-181.
- [12] P. G. Raj and S. Kar, "Design and Development of a Distributed Mobile Sensing Based Crowd Evacuation System: A Big Actor Approach," in *Proc. IEEE 39th Annual COMPSAC*, 2015, pp. 355-360.
- [13] K. M. Yu, C.S. Yu, C.C. Lien, S.T. Cheng, M.Y. Lei, H. P. Hsu and Nancy Tsai, "Intelligent evacuation system integrated with image recognition technology," in *Proc. 8th Int. Conf. UMEDIA*, 2015, pp. 23-28.
- [14] F. Zhu, S. Chen, Z. H. Mao and Q. Miao, "Parallel Public Transportation System and Its Application in Evaluating Evacuation Plans for Large-Scale Activities," *IEEE Trans. on Intelligent Transportation Systems*, vol. 15, no. 4, pp. 1728-1733, Aug. 2014.
- [15] O. Khalid, M. U. S. Khan, Y. Huang, S. U. Khan and A. Zomaya, "EvacSys: A Cloud-Based Service for Emergency Evacuation," *IEEE Cloud Computing*, vol. 3, no. 1, pp. 60-68, Jan.-Feb. 2016.
- [16] M. R. Garey, D. S. Johnson. *Computers and intractability: a guide to the theory of NP-completeness*, CA: New York, 1979, pp. 27-45.
- [17] S. Ferdousi, M. Tornatore, M. F. Habib and B. Mukherjee, "Rapid data evacuation for large-scale disasters in optical Cloud networks," *IEEE/OSA Journal of Optical Communications and Networking*, vol. 7, no. 12, pp. B163-B172, Dec. 2015.
- [18] P. Kirci, "On the Performance of Tabu Search Algorithm for the Vehicle Routing Problem with Time Windows," in *Proc. IEEE 4th Int. Conf. FiCloudW*, 2016, pp. 351-354.
- [19] N. M. Sabri, M. Puteh and M. R. Mahmood, "An overview of Gravitational Search Algorithm utilization in optimization problems," in *Proc. IEEE 3rd ICSET*, 2013, pp. 61-66.
- [20] M. Durak, N. Durak, E. D. Goodman and R. Till, "Optimizing an agent-based traffic evacuation model using genetic algorithms," in *Proc. WSC*, 2015, pp. 288-299.
- [21] M. Gregor, I. Miklóšik and J. Spalek, "Automatic tuning of a fuzzy meta-model for evacuation speed estimation," in *Proc. Cybernetics & Informatics (K&I)*, 2016, pp. 1-6.
- [22] Z. Ye, Y. Yin, X. Zong and M. Wang, "An Optimization Model for Evacuation Based on Cellular Automata and Ant Colony Algorithm," in *Proc. 7th ISCID*, 2014, pp. 7-10.
- [23] O. Khatib, "Real-time obstacle avoidance for manipulators and mobile Robots", *International Journal of Robotics Research*, 1986, pp. 90-98.
- [24] L. Zhou and W. Li, "Adaptive Artificial Potential Field Approach for Obstacle Avoidance Path Planning", in *Proc. 7th ISCID*, 2014, pp. 429-432.
- [25] W. D. Yan, X. L. Zhang, "Study on effect of people's cognitive level on evacuation psychology and behavior in building fire", *Journal of Safety Science and Technology*, vol. 6, no. 5, pp. 108-113, Dec. 2009.